

Tetracoordinate diamidato-bis(phosphanyl) metal systems: Synthesis, characterization, and electrochemical analysis of palladium(II) complexes

Rebecca A. Swanson^a, Brian O. Patrick^b, Michael J. Ferguson^c, Christopher J.A. Daley^{a,*}

^a Department of Chemistry, Western Washington University, Bellingham, WA 98225-9150, United States

^b Department of Chemistry, University of British Columbia, Vancouver, BC, Canada V6T 1Z3

^c Department of Chemistry, University of Alberta, Edmonton, Alta., Canada T6G 2G2

Received 1 December 2006; accepted 6 December 2006

Available online 15 December 2006

Abstract

Square planar diamidato-bis(phosphanyl) palladium(II) complexes have been prepared and characterized. Most products precipitate out of THF solution on reaction of the parent ligand with Pd(OAc)₂ in the presence of 2 equiv. of base at 50 °C overnight. The solution and solid state structure of each complex is reported based on multinuclear NMR and X-ray analyses, respectively. The effects of carboxamido nitrogen coordination on the stabilization of the metal center from reduction were studied using cyclic voltammetry. The irreversible peak reduction potential of each complex was greater by approximately –340 mV to –590 mV as compared to Pd(PPh₃)₂Cl₂ indicating that carboxamido nitrogen coordination protects the Pd(II) center from reduction.

© 2006 Elsevier B.V. All rights reserved.

Keywords: Trost ligand; Palladium complexes; Amidato-metal bonding; Protection from reduction; X-ray crystal structures

1. Introduction

Metal-amidato complexes have attracted much attention over the last couple of decades with studies in areas such as structure and reactivity [1], catalyst development [2], medicinal chemistry [3], and bioinorganic chemistry [4]. Of note, in nature there are a few fascinating systems (Fig. 1) where such coordination occurs including: the P-cluster of nitrogenase [5], the A-cluster of CODH/acetyl Co-A synthase (CODH) [6], and the active site of nitrile hydratase (NHase) [7]. The P-cluster is indispensable for nitrogenase activity as it is believed to participate in the transfer of electrons required to reduce dinitrogen [5,8]. In its oxidized form, the P-cluster is bonded to the enzyme through multiple Cys–S–Fe bonds as well as with an amidato bond from one of the Cys. In the CODH enzyme,

the A-cluster is the active site responsible for interconversion of C₁ carbon species such as CO₂ and CO via redox reactions [6,9]. The exact role of the distal nickel center in the A-cluster remains to be elucidated, however, it is noted that its coordination sphere is similar to that found in NHase being bonded through a peptide backbone Cys–Gly–Cys unit as a diamidato-dithiolate center. NHases are mononuclear non-heme iron(III) or non-corrin cobalt(III) containing enzymes that hydrolyze nitriles to their corresponding amides. In NHase, the mononuclear metal center is bonded in a tetradentate plane via two carboxamido nitrogens and the Cys thiolates from a Cys–Ser–Cys unit where the thiolates have been post-translationally modified to sulfinic and sulfenic units. A third unmodified Cys thiolate binds the metal center below the plane. The stable high oxidation state in NHase is a rare case as transition metal-thiolate species (notably Fe(III)–S systems) are prone to undergo autoreduction [10]; the metal(III) center in NHase shows no redox activity but behaves solely as a

* Corresponding author. Tel.: +1 360 650 3167; fax: +1 360 650 2826.
E-mail address: daley@chem.wvu.edu (C.J.A. Daley).

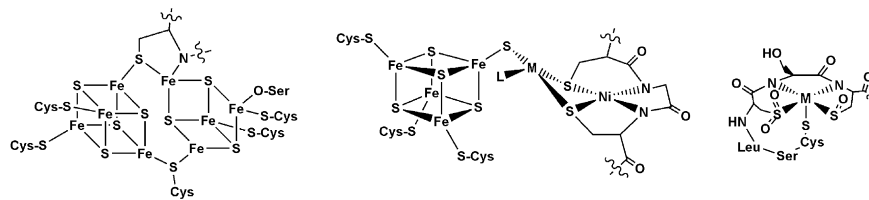


Fig. 1. Structures of complexes containing metal-amidato bonding found in nature. The P-cluster of nitrogenase in the oxidized form (left), the A-cluster of CODH (M = metal; center), and the active site of NHase (right).

Lewis acid [7]. It is the carboxamido nitrogen bonding that has been proposed to protect the metal center from reduction, and thus redox activity, as compared to similar non-coordinated carboxamido nitrogen species [11]. Based on the intriguing examples above, along with the numerous other complexes reported, continued investigation into the properties of metal systems that contain amidato bonding is of great interest.

The Trost ligand (*R,R*)-**1** (Fig. 2) contains carboxamido nitrogens that could coordinate in a manner similar to that of the distal nickel center in CODH and the metal active site in NHase where the thiolate units are substituted for phosphane units. As such, we are interested in examining the properties of metal complexes bound by (*R,R*)-**1** in a tetracoordinate diamidato-bis(phosphanyl) form. We began with the palladium complexes, which are also of interest to the catalytic community as Trost-based palladium systems are well known as highly efficient catalysts for reactions such as enantioselective allylic alkylations. The active catalytic species are believed to be **1-Pd(0)** and **1-Pd(II)(R)(X)** type complexes with the tetracoordinate (*R,R*)-**1-Pd** deemed catalytically inactive [12]. In contrast, the Süß-Fink group has recently reported that the achiral complex **4-Pd** is likely the catalytically active species in Suzuki cross-coupling reactions [13]. Therefore, the complete characterization of diamidato-bis(phosphanyl) palladium complexes is of broad scientific interest. Herein we report on the direct synthesis of (*R,R*)-**1-Pd** and its analogues (*R,R*)-**2-Pd** and (\pm)-**3-Pd**, their structural characterization in solution and the solid state,

their electrochemistry, and compare them to other similar palladium complexes.

2. Experimental

2.1. General

All reactions were performed using standard Schlenk techniques or in a N₂-filled MBraun glovebox. Solvents were purified using an Innovative Technologies Solvent Purification System and were further deoxygenated with N₂-bubbling prior to use. 2-(Diphenylphosphino)benzoic acid (97%; Alfa Aesar), (1*R*,2*R*)-(+)-1,2-diaminocyclohexane-*N,N'*-bis(2'-diphenylphosphinobenzoyl) ((*R,R*)-**1**; 98%, STREM), and (1*R*,2*R*)-(+)-1,2-diaminocyclohexane-*N,N'*-bis(2'-diphenylphosphino-1-naphthoyl) ((*R,R*)-**2**; 94%, STREM) were purchased from suppliers and used without further purification unless stated otherwise. NMR data were obtained on a Varian INOVA 500 MHz spectrometer. The chemical shifts for proton and carbon were referenced to tetramethylsilane (TMS) at 0.00 ppm and the chemical shifts for phosphorus were referenced to 85% H₃PO₄ at 0.00 ppm. X-ray analyses were performed by Dr. Patrick at the University of British Columbia or by Dr. Ferguson at the University of Alberta.

2.2. Synthesis of (\pm)-**3**

The synthesis was modified slightly from that reported by Trost [14]. To a 100 mL side-arm flask were added 2-(diphenylphosphino)benzoic acid (2.0004 g, 6.5310 mmol), dicyclohexylcarbodiimide (1.4820 g, 7.1841 mmol), *N,N*-dimethyl-4-aminopyridine (DMAP; 0.0208 g, 0.1703 mmol), and CH₂Cl₂ (40 mL) to dissolve the solids. The solution was stirred for 35 min then (\pm)-1,2-diphenylethylenediamine (0.6942 g, 3.266 mmol) was added as a solid under a strong flow of N₂. The reaction flask was rinsed with CH₂Cl₂ (4 mL) via cannula to ensure all the diamine was in solution. The chalky yellow mixture was stirred for a further 20 h under N₂. The solution was filtered through a Celite plug (1.5 cm \times 6 cm) into a 100 mL round bottom flask. The Celite was washed with CH₂Cl₂ (2 \times 7 mL) until the eluent was colorless. The solvent was removed under vacuum yielding the crude product as a yellow solid. The solid was purified by column chromatography (silica column 4 cm \times 11 cm) using 1:3 diethyl ether:hexanes (200 mL) followed by 30% ethyl acetate:hex-

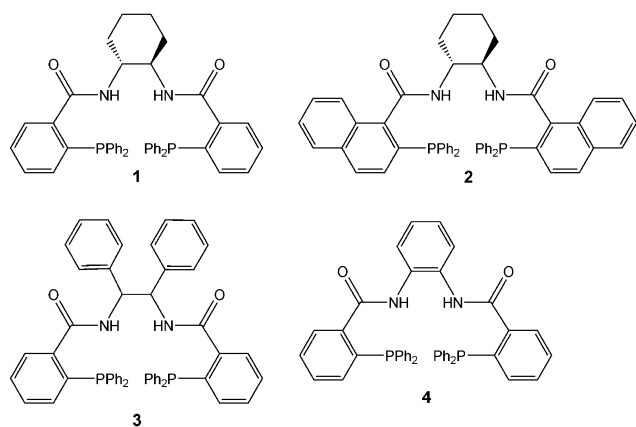


Fig. 2. Ligands with the potential to form tetradentate diamidato-bis(phosphanyl) metal complexes.

anes (800 mL), and 50% ethyl acetate:hexanes (400 mL). After removal of solvent on a rotovap, **3** was collected as a yellow solid that was further recrystallized from CH₂Cl₂:hexanes in a freezer. The off-white solid was collected by filtration in 54.43% yield (1.402 g, 1.777 mmol). ¹H NMR analysis was identical to that reported [7] and (±)-**3** was used without further purification.

2.3. Synthesis of (*R,R*)-**1-Pd**

To a 50 mL side-arm flask was added NaH (0.0195 g, 0.478 mmol; 54% w/w in oil) with a stirbar and THF (10 mL). To this was added a THF (10 mL) solution of **1** (0.150 g, 0.217 mmol) and Pd(OAc)₂ (0.049 g, 0.218 mmol) via cannula. The yellow solution was heated to 50 °C for 17 h. After this time a yellow solid precipitated out of solution. The solution was filtered to yield (*R,R*)-**1-Pd** (0.146 g, 0.184 mmol) in 84.6% yield. ¹H NMR (CDCl₃, 500 MHz) δ 1.25 (m, 2H, H_e), 1.45 (m, 2H, H_b), 1.60 (m, 2H, H_d), 2.49 (br 'd', 2H, H_c), 3.70 (m, 2H, H_a), 6.72 (td, 2H, H_i), 7.11 (m, 4H, *ortho-H*), 7.13–7.23 (m, 14H, H_h + *ortho-H'* + *meta-H,H'*), 7.38 (t, 2H, *para-H'*), 7.42 (t, 2H, *para-H*), 7.51 (t, 2H, H_g), 8.51 (dd, 2H, H_f). ¹³C{¹H} NMR (CDCl₃, 126 MHz) δ 26.27, 31.89, 67.91, 123.86, 124.27, 128.7 (m), 129.16, 129.59, 130.91, 130.95, 131.45, 131.74, 131.98 (m), 133.07 (m), 133.51 (m), 145.37 (m), 167.47. ³¹P{¹H} NMR (CDCl₃, 202 MHz) δ 25.66 (s).

2.4. Synthesis of (*R,R*)-**2-Pd**

In a 50 mL side-arm flask containing a stirbar, NaH (0.0130 g, 0.325 mmol; 54% w/w in oil) and (*R,R*)-**2** (0.112 g, 0.142 mmol) were dissolved in THF (10 mL). To this was added a THF (5 mL) solution of Pd(OAc)₂ (0.0318 g, 0.142 mmol) via cannula from a 25 mL side-arm flask. The stirred yellow solution was heated to 50 °C for 24 h. Note: no solid precipitates out of solution. The solvent was removed under vacuum to yield (*R,R*)-**2-Pd** (0.113 g, 0.126 mmol) in 89.1% yield. ¹H NMR analysis of the product showed no visible impurities but the product was crystallized from CH₂Cl₂:Et₂O prior to use in cyclic voltammetry studies. ¹H NMR (CDCl₃, 500 MHz) δ 1.14 (m, 2H, H_b), 1.52 (m, 2H, H_e), 1.75 (m, 2H, H_d), 3.25 (br 'd', 2H, H_c), 3.94 (m, 2H, H_a), 6.49 (t, 2H, H_i), 7.04–7.14 (m, 8H, *ortho-H'* + *meta-H'*), 7.22–7.28 (m, 4H, *meta-H*), 7.35 (t, 2H, *para-H*), 7.40 (t, 2H, *para-H'*), 7.46–7.58 (m, 10H, H₂ + H₃ + H_h + *ortho-H*), 7.71 (d, 2H, H₄), 8.59 (d, 2H, H₁). ¹³C{¹H} NMR (CDCl₃, 126 MHz) δ 25.86, 31.43, 68.82, 123.42 (m), 125.60, 127.28, 127.33, 127.60, 127.98, 128.18, 128.42 (m), 128.60–128.88 (m), 130.75, 131.51 (m), 131.69, 133.26 (m), 134.91 (m), 135.19, 147.97 (m), 176.74 (m). ³¹P{¹H} NMR (CDCl₃, 202 MHz) δ 23.66 (s).

2.5. Synthesis of (±)-**3-Pd**

Compound (±)-**3-Pd** was synthesized in a similar manner to **1-Pd** using (±)-**3** (0.1382 g, 0.1752 mmol), NaH

(0.0163 g, 0.408 mmol; 54% w/w in oil), and Pd(OAc)₂ (0.0393 g, 0.175 mmol). Compound (±)-**3-Pd** was obtained in 92.7% yield (0.145 g, 0.162 mmol). ¹H NMR (CDCl₃, 500 MHz) δ 6.42 (dd, 2H, H_i), 6.57 (d, 2H, H_a), 6.65 (dd, 4H, *ortho-H*), 6.81 (t, 4H, H_m), 7.12 (m, 8H, *para-H* + *meta-H_b* + *para-H_b*), 7.18 (t, 2H, H_h), 7.32 (t, 4H, *meta-H'*), 7.37 (m, 4H, *ortho-H_b*), 7.50 (m, 4H, H_g + *para-H'*), 7.58 (dd, 4H, *ortho-H'*), 8.69 (dd, 2H, H_f). ¹³C{¹H} NMR (CDCl₃, 126 MHz) δ 125.46 (m), 125.55, 127.30, 127.79, 128.50, 128.83, 130.18, 131.60, 131.75, 132.02, 132.28, 133.03, 135.91, 142.93, 143.27, 165.43. ³¹P{¹H} NMR (CDCl₃, 202 MHz) δ 26.49 (s).

2.6. X-ray crystallography

The crystal data for (*R,R*)-**1-Pd**, (*R,R*)-**2-Pd**, and (±)-**3-Pd** are collected in Table 1. Crystals of (*R,R*)-**1-Pd**, (*R,R*)-**2-Pd**, and (±)-**3-Pd** suitable for X-ray structure determination were obtained by vapor diffusion of diethyl ether into a concentrated solution of the compound of interest in CH₂Cl₂.

Data for (*R,R*)-**1-Pd** and (*R,R*)-**2-Pd** were collected at the University of British Columbia on a Bruker X8 APEX CCD diffractometer utilizing graphite monochromated Mo Kα radiation at –100 °C. Unit cell parameters were obtained from a least-squares refinement of the setting angles of 6793 reflections ((*R,R*)-**1-Pd**) or 7498 reflections ((*R,R*)-**2-Pd**) from the data collection. The space group was determined to be *P*2₁2₁2₁ ([No. 19]) for both (*R,R*)-**1-Pd** and (*R,R*)-**2-Pd**. The data were corrected for absorption effects using the multi-scan technique (SADABS) [15]. See Table 1 for a summary of the crystal data and X-ray data collection information. The structures were solved by direct methods [16] and refined using full-matrix least squares [17] of F². All refinements were performed using the SHELXTL crystallographic software package [18]. The non-H atoms were treated anisotropically. Hydrogen atoms were assigned positions on the basis of the geometries of their attached carbon atoms and were given thermal parameters 20% greater than those of the attached carbons. For (*R,R*)-**1-Pd**, the final model refined to values of R₁(F) = 0.027 (for 7936 data with F_o² ≥ 2 ∑(F_o²)) and wR₂(F²) = 0.0660 (for all 8535 independent data). For (*R,R*)-**2-Pd**, the final model refined to values of R₁(F) = 0.043 (for 6982 data with F_o² ≥ 2 ∑(F_o²)) and wR₂(F²) = 0.097 (for all 7745 independent data).

Data for (±)-**3-Pd** was collected at the University of Alberta on a Bruker Platform/SMART 1000 CCD diffractometer using Mo Kα radiation at –80 °C. Unit cell parameters were obtained from a least-squares refinement of the setting angles of 8136 reflections from the data collection. The space group was determined to be *P*2₁/*n* (an alternate setting of *P*2₁/*c* [No. 14]). The data were corrected for absorption through use of the program SADABS [19]. See Table 1 for a summary of crystal data and X-ray data collection information. The structures were solved using direct methods (SHELXS-86) [20], and refinement was completed

Table 1
Selected crystallographic data for (*R,R*)-**1-Pd**, (*R,R*)-**2-Pd**, and (\pm)-**3-Pd**^a

	(<i>R,R</i>)- 1-Pd	(<i>R,R</i>)- 2-Pd	(\pm)- 3-Pd
Formula	C ₄₄ H ₃₈ N ₂ O ₂ P ₂ Pd	C ₅₂ H ₄₂ N ₂ O ₂ P ₂ Pd · CH ₂ Cl ₂	C ₅₂ H ₄₀ N ₂ O ₂ P ₂ Pd · CH ₂ Cl ₂
Formula weight (g/mol)	795.10	980.14	978.13
<i>a</i> (Å)	9.7744 (3)	11.9129 (4)	11.0579 (7)
<i>b</i> (Å)	17.5108 (6)	13.2944 (4)	19.6816 (12)
<i>c</i> (Å)	21.0956 (7)	28.6030 (8)	20.7039 (12)
α (°)	90.0	90.00	90.0
β (°)	90.0	90.00	95.747 (1)
γ (°)	90.0	90.00	90.0
<i>V</i> (Å ³)	3610.7 (2)	4530.0(2)	4483.3 (5)
<i>Z</i>	4	4	4
Space group	<i>P</i> 2 ₁ 2 ₁ (#19)	<i>P</i> 2 ₁ 2 ₁ (#19)	<i>P</i> 2 ₁ / <i>n</i> (#14)
Crystal system	orthorhombic	orthorhombic	monoclinic
ρ_{calc} (g/cm ³)	1.463	1.437	1.449
<i>T</i> (K)	173	173	193
μ (Mo K α) (mm ⁻¹)	0.644	0.643	0.649
Total reflections	37726	24207	34152
2 θ Range (°)	3.02–55.60	3.38–50.00	2.86–52.76
Unique reflections	8535	7745	9171
Parameters	460	559	559
Flack χ	–0.04 (1)	–0.02 (3)	
<i>R</i> ₁ ^b , <i>wR</i> ₂ ^c	0.027, 0.066	0.043, 0.097	0.0299, 0.0855
<i>S</i> ^b	1.07	1.05	1.051

^a See CCDC 629352, 629353, and 629354 deposition files for more information.

^b $R_1 = \sum ||F_o| - |F_c|| / \sum |F_o|$, $I \geq 2\sigma(I)$; $wR_2 = \{ \sum [w(F_o^2 - F_c^2)]^2 / \sum [w(F_o^2)]^2 \}^{1/2}$, all data.

^c $S = \{ \sum [w(F_o^2 - F_c^2)]^2 / (n - p) \}^{1/2}$.

using the program SHELXL-93 [21]. Hydrogen atoms were assigned positions on the basis of the geometries of their attached carbon atoms and were given thermal parameters 20% greater than those of the attached carbons. For (\pm)-**3-Pd**, the final model refined to values of $R_1(F) = 0.0299$ (for 8211 data with $F_o^2 \geq 2 \sum (F_o^2)$) and $wR_2(F^2) = 0.0855$ (for all 9171 independent data).

2.7. Electrochemistry

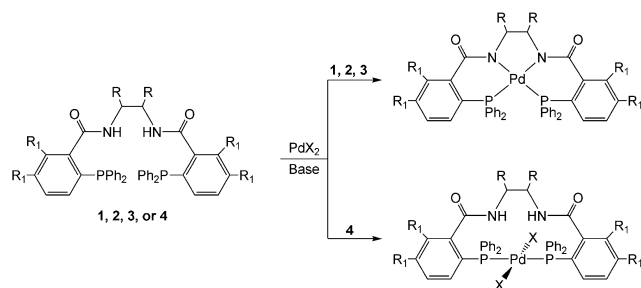
Measurements were carried out at 20 ± 2 °C using a standard three-electrode arrangement with a platinum wire as the counter electrode and a Ag/AgCl double-junction reference electrode in CH₂Cl₂ containing 0.1 M (Bu₄N)(PF₆) supporting electrolyte. All potentials are quoted with respect to this electrode. Cyclic voltammograms (500 mV/s) were recorded with a BAS CV-50 W (BioAnalytical System Instruments) system using a glassy carbon working electrode and 0.15–0.25 mM solutions of the sample in CH₂Cl₂ electrolyte solution. Oxygen was removed from each sample by purging the solutions with high-purity nitrogen.

3. Results and discussion

3.1. Synthesis and characterization

Palladium complexes of the Trost ligand **1** are of interest as they may be, or may model, active catalytic species in enantioselective palladium-catalyzed reactions such as allylic alkylations. The coordination modes of **1** with palla-

dium are of interest as the similar ligand **4** (Fig. 2) developed by Burger et al. was found to only form the bis(phosphanyl) palladium(II) complex (**4-PdCl₂**) [22] where the phosphanes coordinate trans to each other and the carboxamido nitrogens do not participate in the bonding (Scheme 1) unless high heat and a stronger base was used, in which case the **4-Pd** complex can be formed [13]. Even on reaction of **4-PdCl₂** with excess NEt₃ as base, formation of the corresponding diamidato-bis(phosphanyl) palladium(II) complex (**4-Pd**) was not observed at room temperature [22]. In contrast, **1** has been shown to form a cis coordinate bis(phosphanyl) palladium(0) complex [12], believed to be the active coordination mode in numerous enantioselective catalyzed reactions, as well as the diamidato-bis(phosphanyl) palladium(II) complex **1-Pd** [12,23] that is reported to be catalytically inactive for the aforementioned reactions. The first report of the formation of **1-Pd** was on opening a solution of the bis(phosphanyl)



Scheme 1.

palladium(0) complex to air [12]. More recently, Campos et al. obtained **1-Pd** as a byproduct on workup of a catalytic asymmetric allylic alkylation reaction as confirmed by its X-ray structure [23]. However, the isolation, yield, and further characterization of **1-Pd** were not reported in either case. In order to investigate this complex further, we set forth to develop a straightforward synthesis of (*R,R*)-**1-Pd** along with its analogues (*R,R*)-**2-Pd** and (\pm)-**3-Pd**.

We successfully synthesized (*R,R*)-**1-Pd** on reaction of (*R,R*)-**1** with Pd(OAc)₂ in THF at 50 °C for 17 h. The product (*R,R*)-**1-Pd** precipitates out of solution and can be isolated by filtration in high yield (Scheme 1: 84.6%). It is noted that unlike the reactivity of **4**, reaction of (*R,R*)-**1** with Pd(OAc)₂ in CH₂Cl₂ at room temperature did form some of the desired (*R,R*)-**1-Pd** when no base was added, however the reaction was not clean as several other unidentified complexes were also present. Furthermore, reaction of (*R,R*)-**1** with Pd(OAc)₂ in THF at room temperature for 24 h in the presence of base did precipitate (*R,R*)-**1-Pd** but in only a modest quantity (28.7% yield). The complex (*R,R*)-**1-Pd** was formed cleanly and in the best yield when base was added and the mixture was heated.

A possibility for the lack of the amidato bonding of **4** to the Pd(II) center at room temperature may be the nature of the carboxamido nitrogens themselves. The nitrogens of **1–3** are bonded to aliphatic carbons whereas they are bonded to an aromatic ring in **4**. While the lack of carboxamido nitrogen coordination may be a result of the less nucleophilic nature of the carboxamido nitrogens in **4**, the fact that the analogous diamidato bis(phosphanyl) platinum(II) complex (**4-Pt**) [23] is formed in the absence of base suggests that the nucleophilic nature of the nitrogens is not the primary factor to coordination. As noted, while (*R,R*)-**1-Pd** was formed without heat in the presence of base and even in the absence of base, the most efficient synthesis of (*R,R*)-**1-Pd** required heating the solution in base. The byproduct (*R,R*)-**1-Pd** reported by Campos [23] was formed after prolonged heating of a basic ethanol solution and the achiral analogue **4-Pd** reported by the Süss-Fink [13] group was only isolated on heating a toluene solution in the presence of K₂CO₃. These reports further support our theory that while the nucleophilic nature of the carboxamido nitrogens may be a factor, heat is the key component to carboxamido nitrogen coordination to the Pd(II) center. While Trost reported the clean formation of **1-Pd** at room temperature, the reaction occurred on exposure of the bis(phosphanyl) coordinated Pd(0) complex of **1** to air. The resultant reaction pathway involves oxidation of Pd(0) to Pd(II) that may provide a lower barrier to the formation of **1-Pd**. The palladium complexes of (*R,R*)-**2** and (\pm)-**3** were also synthesized to further examine the properties of these structurally related ligands. Complex (\pm)-**3-Pd** precipitated out of the THF solution overnight (92.7% yield) like that of (*R,R*)-**1-Pd** however (*R,R*)-**2-Pd** remained in solution as the naphthyl backbone increased its solubility in THF. Complex (*R,R*)-**2-Pd** was isolated on removal

of THF and further purified by crystallization from CH₂Cl₂:Et₂O (89.1% yield).

3.2. Solution structure

Complex (*R,R*)-**1-Pd** was characterized in solution by multinuclear NMR analyses. Two immediate features noted in the ¹H NMR spectrum (Fig. 3) were the disappearance of the amide protons, strongly indicating coordination of the carboxamido nitrogens, and a signature peak that appeared at 8.51 ppm. The latter peak is the only signal observed down-field of 8 ppm and was an indication of successful coordination with all the complexes. In solution, (*R,R*)-**1-Pd** has C₂-symmetry based on the number of ¹H NMR signals and integration and is further confirmed by the single peak observed in the ³¹P{¹H} NMR spectrum at 25.66 ppm (singlet). All ¹H NMR signals were assigned based on multidimensional NMR analyses including HMQC, HMBC, COSY, NOESY, and ROESY. Protons H_a were readily identified (Fig. 3) at 3.70 ppm as they are the only protons expected in this region. The ¹H NMR signal at 6.72 ppm was assigned as H_i based on integration of the signal and the loss of coupling observed in the ¹H{³¹P} NMR spectrum. The remaining cyclohexyl backbone protons H_b–H_d and the remaining aromatic backbone protons H_f–H_j were then assigned via analysis of the COSY, HMBC, and NOESY spectra with respect to the H_a and H_i signals, respectively. The signature peak at 8.51 ppm corresponds to H_f, which was confirmed from its cross-coupling to the carbonyl carbon in the HMBC spectrum. Assignment of the auxiliary phenyl protons on the phosphorus arms was then completed [24].

Similarly to (*R,R*)-**1-Pd**, complexes (*R,R*)-**2-Pd** and (\pm)-**3-Pd** were characterized in solution by multinuclear NMR analysis; both display C₂-symmetry in solution based on the number and integration of the ¹H NMR signals (Fig. 3) as well as the single ³¹P{¹H} NMR signals observed for each complex ((*R,R*)-**2-Pd**, 23.66 ppm; (\pm)-**3-Pd**, 26.49 ppm). The ¹H NMR spectra lacked the N–H proton signals indicating coordination of the carboxamido nitrogens, and each complex had the characteristic ¹H signal at ~ 8.5 ppm indicating tetradentate coordination similar to that found with (*R,R*)-**1-Pd**. The latter signals were identified as H_f for (\pm)-**3-Pd** from COSY, HMBC, and NOESY analyses based on the signal H_i that was assigned from integration and ¹H{³¹P} NMR analyses. H_i for (*R,R*)-**2-Pd** was assigned in a similar manner and had the added identifier of a strong NOE to the cyclohexyl backbone protons H_c. The backbone phenyl group protons (on the ethylenediamine fragment) of (\pm)-**3-Pd** were distinguished from those of the phosphane via a strong NOE between H_a and *ortho*-H_b. Based on these data, the complexes were identified as C₂-symmetric diamidato-bis(phosphanyl) square planar complexes. Analysis of the solid state structures of each complex was performed in order to compare them to each other and with their solution structures.

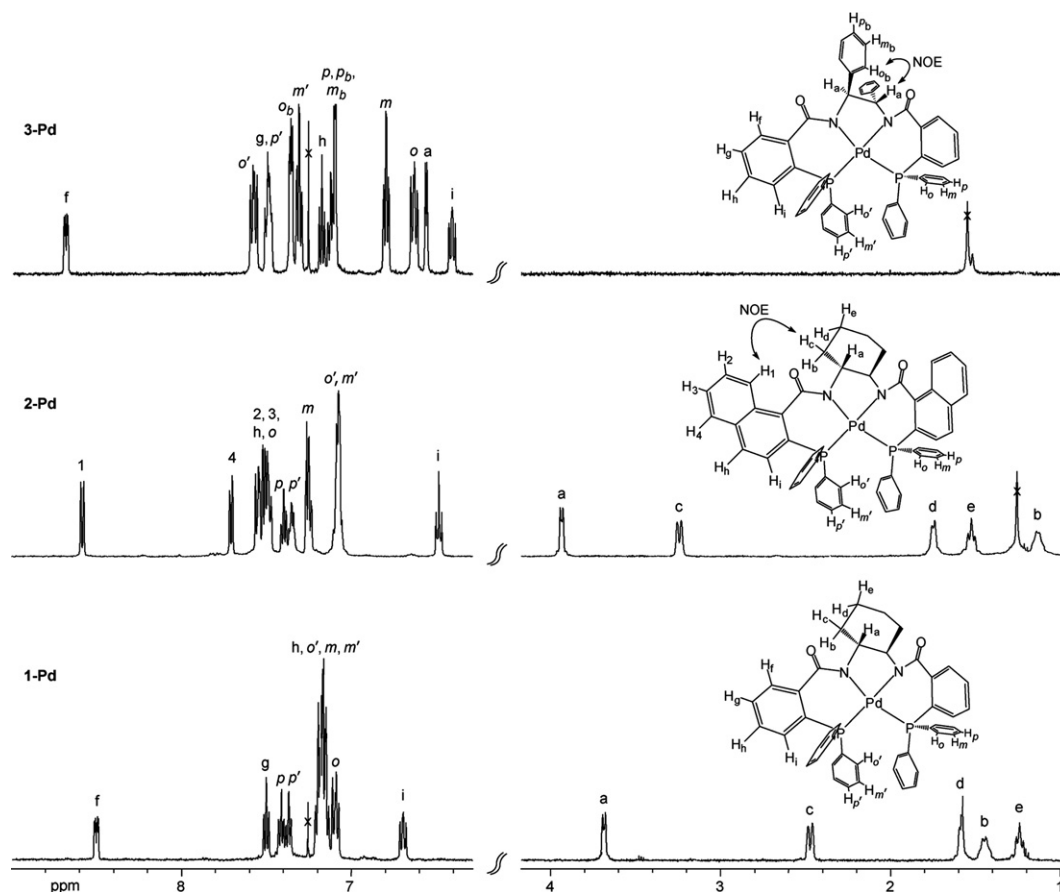


Fig. 3. ^1H NMR spectra of (R,R) -**1-Pd**, (R,R) -**2-Pd**, and (\pm) -**3-Pd** in CDCl_3 . Only the (S,S) -**3-Pd** enantiomer is depicted for assignment purposes, but the product is racemic. Proton assignments are as denoted except for the residual CHCl_3 and water signals which are denoted with an 'x'. The region between 4.2 and 6.2 ppm contains no peaks and has been omitted for clarity.

3.3. Solid state structure

The products were characterized in the solid state by X-ray crystallography using crystals obtained via diethyl ether vapor diffusion into a concentrated solution of (R,R) -**1-Pd**, (R,R) -**2-Pd**, or (\pm) -**3-Pd** in CH_2Cl_2 (Tables 1

and 2; Fig. 4). While the structure of (R,R) -**1-Pd** has been reported, we report our structure here for completeness to the series of complexes in this manuscript and because of the differences noted from the original report. Of experimental note, our structure was collected at -100°C and the unit cell volume was determined to be 3610.7 \AA^3 while

Table 2
Selected bond distances (\AA) and angles ($^\circ$) for complexes (R,R) -**1-Pd**, (R,R) -**2-Pd**, (\pm) -**3-Pd**

(R,R) - 1-Pd		(R,R) - 2-Pd		(\pm) - 3-Pd	
Pd–N(1)	2.0674(18)	Pd–N(1)	2.089(4)	Pd–N(1)	2.0523(17)
Pd–N(2)	2.0687(16)	Pd–N(2)	2.073(4)	Pd–N(2)	2.0560(17)
Pd–P(1)	2.2525(5)	Pd–P(1)	2.2793(14)	Pd–P(1)	2.2480(5)
Pd–P(2)	2.2549(6)	Pd–P(2)	2.2532(12)	Pd–P(2)	2.2389(5)
N(1)–C(1)	1.493(3)	N(1)–C(x)	1.483(6)	N(1)–C(1)	1.480(3)
N(2)–C(6)	1.485(2)	N(2)–C(y)	1.474(6)	N(2)–C(2)	1.480(3)
C(1)–C(6)	1.527(3)	C(1)–C(6)	1.522(7)	C(1)–C(2)	1.524(3)
N(1)–Pd–N(2)	83.94(7)	N(1)–Pd–N(2)	83.55(15)	N(1)–Pd–N(2)	84.09(7)
N(1)–Pd–P(1)	90.86(5)	N(1)–Pd–P(1)	88.21(11)	N(1)–Pd–P(1)	87.47(5)
N(1)–Pd–P(2)	166.99(5)	N(1)–Pd–P(2)	171.47(12)	N(1)–Pd–P(2)	171.07(5)
N(2)–Pd–P(1)	174.70(5)	N(2)–Pd–P(1)	169.59(12)	N(2)–Pd–P(1)	171.35(5)
N(2)–Pd–P(2)	83.05(5)	N(2)–Pd–P(2)	89.27(11)	N(2)–Pd–P(2)	88.40(5)
P(1)–Pd–P(2)	102.14(2)	P(1)–Pd–P(2)	98.39(5)	P(1)–Pd–P(2)	100.17(2)
N(1)–C(1)–C(6)	106.95(17)	N(1)–C(1)–C(6)	106.1(4)	N(1)–C(1)–C(2)	106.08(16)
N(2)–C(6)–C(1)	108.92(17)	N(2)–C(6)–C(1)	110.6(4)	N(2)–C(2)–C(1)	107.06(17)

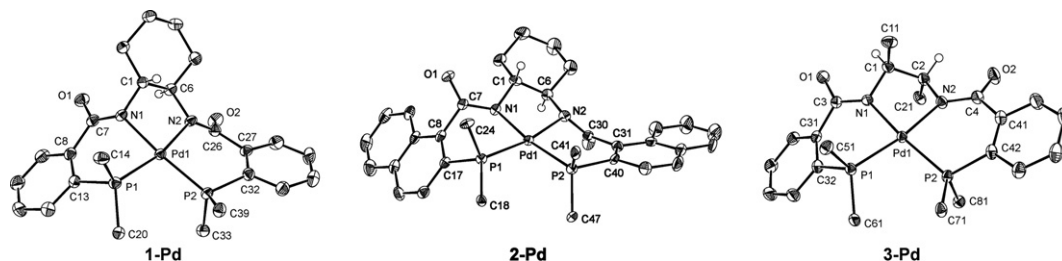


Fig. 4. ORTEP plot at 50% probability level of *(R,R)*-**1-Pd**, *(R,R)*-**2-Pd**, and *(S,S)*-**3-Pd**. Note that **3-Pd** is racemic and the unit cell contains two molecules of *(S,S)*-**3-Pd** and two of *(R,R)*-**3-Pd** but only one enantiomer is shown for clarity. The ancillary phenyl groups and hydrogen atoms (except those on the carbon atoms adjacent to the amide nitrogens) are omitted for clarity. In the case of *(R,R)*-**2-Pd** and (\pm) -**3-Pd** a molecule of CH_2Cl_2 co-crystallized but it is omitted for clarity.

the Campos structure [23] was collected at room temperature and the unit cell volume was determined to be 3600.13 \AA^3 . This is an interesting structural observation as normally the cell volume decreases with decreasing temperature yet the opposite is observed. Another difference is that while they are close, all the Pd–X (X = N or P) bond lengths of our structure are longer ($>3\sigma$) than those of the Campos structure. Finally, our structure refined to a better *R*-factor of 2.65% as compared to 4.69% reported by Campos [25]. The complexes are all square planar about the palladium as confirmed by the summation of the bond angles between the coordinating atoms ($\text{P}(1)\text{--Pd--N}(1) + \text{N}(1)\text{--Pd--N}(2) + \text{N}(2)\text{--Pd--P}(2) + \text{P}(2)\text{--Pd--P}(1) = 360^\circ$ ideally for square planar; *(R,R)*-**1-Pd** = $360.0(2)^\circ$; *(R,R)*-**2-Pd** = $359.4(4)^\circ$; (\pm) -**3-Pd** = $360.1(2)^\circ$). It is noted that (\pm) -**3-Pd** maintains pseudo- C_2 -symmetry in the solid state while the C_2 -symmetry is broken in *(R,R)*-**1-Pd** and *(R,R)*-**2-Pd** as the cyclohexyl backbone is out of the square plane set by the phosphorus, nitrogen, and palladium atoms. Within each complex, the Pd–N(1) and Pd–N(2) bond lengths are equivalent (within 3σ) as are the Pd–P(1) and Pd–P(2) bond lengths for complex *(R,R)*-**1-Pd** (Table 2). The Pd–P(1) versus Pd–P(2) bond lengths of *(R,R)*-**2-Pd** ($\Delta \sim 0.02 \text{ \AA}$) and (\pm) -**3-Pd** ($\Delta \sim 0.01 \text{ \AA}$) are slightly asymmetric. Overall, the bond lengths in each complex are in the range of those reported for similar complexes including **4-Pd** [13].

3.4. Electrochemical analysis

Studies of active site synthetic analogues and the native enzyme of nitrile hydratase have shown that amidato coordination protects the Fe(III) (and Co(III)) mononuclear metal center from reduction even in the presence of coordinated thiolate groups [7]. In contrast, higher oxidation state transition metal complexes with coordinated thiolate ligands generally undergo autoreduction [10]. Furthermore, amidato coordination has been shown to stabilize the higher oxidation states of various metals in the absence of coordinated thiolates [11]. The reason for the increased stability has been associated with the strong σ -donor nature of the carboxamido nitrogen anion. To determine if the amidato coordination in *(R,R)*-**1-Pd**, *(R,R)*-**2-Pd**, and (\pm) -**3-Pd** further stabilized the Pd(II) center the electro-

chemistry of the complexes was examined via cyclic voltammetry to determine their peak reduction potentials (Table 3). As a baseline complex $\text{Pd}(\text{PPh}_3)_2\text{Cl}_2$ was chosen as it contains two triarylphosphane ligands similar to *(R,R)*-**1-Pd**, *(R,R)*-**2-Pd**, and (\pm) -**3-Pd** but has no metal-amidato bonding [26]. Cyclic voltammograms of *(R,R)*-**1**, *(R,R)*-**2**, and (\pm) -**3** in the absence and in the presence of base were run in order to determine if the ligands themselves (free or deprotonated) have any electrochemical features in the range analyzed with the palladium complexes. There were no peaks observed for any of them on sweeping the range from 0 V to -2.2 V to 1.0 V and back to 0 V (versus Ag/AgCl) in CH_2Cl_2 solution containing 0.1 M $(\text{Bu}_4\text{N})(\text{PF}_6)$ as electrolyte. Under the same conditions, $\text{Pd}(\text{PPh}_3)_2\text{Cl}_2$ has an irreversible peak reduction potential at -1.25 V [27]. By comparison, each of the amidato complexes has a higher peak reduction potential in the order of -1.59 V (*(R,R)*-**2-Pd**), -1.76 V (*(R,R)*-**1-Pd**), and -1.84 V ((\pm) -**3-Pd**). Based on the silent voltammograms of the free and deprotonated ligands, the reduction peaks observed are due to the reduction of the metal center. It is noted that while $\text{Pd}(\text{PPh}_3)_2\text{Cl}_2$ showed a clear irreversible reduction peak, complexes *(R,R)*-**1-Pd**, *(R,R)*-**2-Pd**, and (\pm) -**3-Pd** had quasi-reversible reduction peaks. The latter quasi-reversible assignment is based on the -50 mV to -66 mV shift in the peak reduction potential of the complexes on changing the scan rates from 100 mV/s to 600 mV/s . On comparison of $\text{Pd}(\text{PPh}_3)_2\text{Cl}_2$ to *(R,R)*-**1-Pd**, *(R,R)*-**2-Pd**, and (\pm) -**3-Pd**, the results indicate that the amidato bonding does protect the Pd(II) center from reduction. This stabilization of the Pd(II) state may be contributing to the inactivity of *(R,R)*-**1-Pd** (and *(R,R)*-**2-Pd** and (\pm) -**3-Pd**) as

Table 3
Reduction peak potentials (E_p) of Pd(II) complexes from cyclic voltammetry studies^a

Entry	Compound	E_p reduction ^b (V)
1	1-Pd	-1.76^c
2	2-Pd	-1.59^c
3	3-Pd	-1.84^c
4	$\text{Pd}(\text{PPh}_3)_2\text{Cl}_2$	-1.25

^a Voltammograms were measured at 500 mV/s in CH_2Cl_2 solutions containing 0.1 M $(\text{Bu}_4\text{N})(\text{PF}_6)$ as electrolyte.

^b Measured vs. Ag/AgCl reference electrode.

^c Quasi reversible reduction peak observed.

active catalysts in allylic alkylation reactions as the complexes are not easily reduced back to Pd(0), which is required to complete the catalytic cycle. These results confirm that carboxamido nitrogen coordination to a metal significantly alters the electronic properties of the metal complex, which includes the protection of the metal center from reduction.

4. Conclusions

We have reported the synthesis of three diamidato-bis(phosphanyl) palladium(II) complexes that readily coordinate in a square planar tetradentate fashion. Each complex has been characterized in solution by NMR and in the solid state by X-ray crystallographic analyses and their electrochemistry has been studied using cyclic voltammetry. The latter allowed for the analysis of the effect carboxamido nitrogen bonding to Pd(II) has on stabilizing the complex from reduction. As observed with other high oxidation state metal complexes, the carboxamido nitrogen bonding to the Pd(II) centers in (*R,R*)-**1-Pd**, (*R,R*)-**2-Pd**, and (\pm)-**3-Pd** protected the complexes from reduction as noted by the increased peak reduction potentials that were approximately -340 mV to -590 mV greater in comparison to similar bis(phosphanyl) Pd(II) complexes that do not contain amidato ligation.

Acknowledgements

We are pleased to acknowledge the financial support of the Research Corporation (Cottrell College CC6100) and the Bureau for Faculty Research at Western Washington University. All NMR data were recorded on a Varian INOVA 500 MHz spectrometer that was funded by the National Science Foundation (NSF-MRI #0216604). We thank Dr. James Vyvyan of Western Washington University for supplying (\pm)-1,2-diphenylethylenediamine.

Appendix A. Supplementary material

CCDC 629352, 629353, and 629354 contain the supplementary crystallographic data for this paper. The data can be obtained free of charge via <http://www.ccdc.cam.ac.uk/conts/retrieving.html>, or from the Cambridge Crystallographic Data Centre, 12 Union Road, Cambridge CB2 1EZ, UK; fax: (+44) 1223-336-033; or e-mail: depos@ccdc.cam.ac.uk. Supplementary data associated with this article can be found, in the online version, at [doi:10.1016/j.ica.2006.12.011](https://doi.org/10.1016/j.ica.2006.12.011).

References

- [1] (a) Examples of complexes and reactivity studies: R.K. Thomson, F.E. Zahariev, Z. Zhang, B.O. Patrick, Y.A. Wang, L.L. Schafer, *Inorg. Chem.* 44 (2005) 8680; (b) E. Hevia, J. Pérez, V. Riera, *Organometallics* 22 (2003) 257; (c) B.-H. Huang, T.-L. Yu, Y.-L. Huang, B.-T. Ko, C.-C. Lin, *Inorg. Chem.* 41 (2002) 2987;
- (d) V.Y. Kukushkin, A.J.L. Pombeiro, *Chem. Rev.* 102 (2002) 1771;
- (e) H. Nagao, T. Hirano, N. Tsuboya, S. Shiota, M. Mukaida, T. Oi, M. Yamasaki, *Inorg. Chem.* 41 (2002) 6267;
- (f) A.T. Vlahos, E.I. Tolis, C.P. Raptopoulou, A. Tsohos, M.P. Sigalas, A. Terzis, T.A. Kabanos, *Inorg. Chem.* 39 (2000) 2977;
- (g) A. Erxleben, A. Albinati, B. Lippert, *J. Chem. Soc., Dalton Trans.* (1996) 1823;
- (h) F.A. Cotton, J. Lu, T. Ren, *Polyhedron* 13 (1994) 807;
- (i) T. Maetzke, D. Seebach, *Organometallics* 9 (1990) 3032;
- (j) A.M. Dennis, J.D. Korp, I. Bernal, R.A. Howard, J.L. Bear, *Inorg. Chem.* 22 (1983) 1522;
- (k) J. Duncan, T. Malinski, T.P. Zhu, Z.S. Hu, K.M. Kadish, J.L. Bear, *J. Am. Chem. Soc.* 104 (1982) 5507.

- [2] (a) Selected catalyst examples: T.E. Patten, C. Troeltzsch, M.M. Olmstead, *Inorg. Chem.* 44 (2005) 9197; (b) P. Pelagatti, M. Carcelli, F. Calbani, C. Cassi, L. Elviri, C. Pelizzi, U. Rizzotti, D. Rogolino, *Organometallics* 24 (2005) 5836; (c) L.D. McPherson, M. Drees, S.I. Khan, T. Strassner, M.M. Abu-Omar, *Inorg. Chem.* 43 (2004) 4036; (d) S. Battacharya, K. Snehalatha, V.P. Kumar, *J. Org. Chem.* 68 (2003) 2741; (e) B.Y. Lee, X. Bu, G.C. Bazan, *Organometallics* 20 (2001) 5425; (f) S. Nishino, M. Kunita, Y. Kani, S. Ohba, H. Matsushima, T. Tokii, Y. Nishida, *Inorg. Chem. Commun.* 3 (2000) 145; (g) Y. Ishikawa, S. Ito, S. Nishino, S. Ohba, Y. Nishida, *Z. Naturforsch. C: J. Biosci.* 53 (1998) 378.
- [3] F.P. Intini, M. Lanfranchi, G. Natile, C. Pacifico, A. Tiripicchio, *Inorg. Chem.* 35 (1996) 1715.
- [4] (a) A. Ghosh, F.T. de Oliveira, T. Yano, T. Nishioka, E.S. Beach, I. Kinoshita, E. Münck, A.D. Ryabov, C.P. Horowitz, T.J. Collins, *J. Am. Chem. Soc.* 127 (2005) 2505; (b) M. Michel Meyer, L. Frémond, E. Espinosa, R. Guillard, Z. Ou, K.M. Kadish, *Inorg. Chem.* 43 (2004) 5572; (c) W. Henderson, A.G. Oliver, C.E.F. Rickard, *Inorg. Chim. Acta* 307 (2000) 144; (d) S.M. Redmore, C.E.F. Rickard, S.J. Webb, L.J. Wright, *Inorg. Chem.* 36 (1997) 4743; (e) R.H. Holm, P. Kennepohl, E.I. Solomon, *Chem. Rev.* 7 (1996) 2239.
- [5] S.M. Mayer, D.M. Lawson, C.A. Gormal, S.M. Roe, B.E. Smith, *J. Mol. Biol.* 292 (1999) 871.
- [6] G.H. Loew, D.L. Harris, *Chem. Rev.* 100 (2000) 407.
- [7] (a) J.A. Kovacs, *Chem. Rev.* 104 (2004) 825; (b) T.C. Harrop, P.K. Mascharak, *Acc. Chem. Res.* 37 (2003) 253; (c) M. Odaka, M. Tsujimura, I. Endo, *RIKEN* 41 (2001) 58.
- [8] M.C. Jeannine, J. Christiansen, D.R. Dean, L.C. Seefeldt, *Biochemistry* 38 (1999) 5779.
- [9] C.G. Riordan, *J. Biol. Inorg. Chem.* 9 (2004) 509.
- [10] (a) L.E. Maelia, M. Millar, S.A. Koch, *Inorg. Chem.* 31 (1992) 4594; (b) M. Millar, J.F. Lee, R. Fikar, *Inorg. Chim. Acta* 243 (1996) 333; (c) T. Herskovitz, B.V. Depamphilis, W.O. Gillum, R.H. Holm, *Inorg. Chem.* 14 (1975) 1426.
- [11] T.J. Collins, *Acc. Chem. Res.* 27 (1994) 279, and references therein.
- [12] B.M. Trost, B. Breit, M.G. Organ, *Tetrahedron Lett.* 35 (1994) 5817.
- [13] L. Chahen, L. Karmazin-Brelot, G. Süß-Fink, *Inorg. Chem. Commun.* 9 (2006) 1151.
- [14] B.M. Trost, D.L. Van Vranken, C. Bingel, *J. Am. Chem. Soc.* 114 (1992) 9327.
- [15] SADABS, Bruker Nonius area detector scaling and absorption correction – V2.10, Bruker AXS Inc., Madison, Wisconsin, USA, 2003.
- [16] SIR97: A. Altomare, M.C. Burla, M. Camalli, G.L. Casciarano, C. Giacovazzo, A. Guagliardi, A.G.G. Moliterni, G. Polidori, R. Spagna, *J. Appl. Cryst.* 32 (1999) 115.
- [17] Least squares function minimized: $w(F_o^2 - F_c^2)^2$.
- [18] SHELXTL Version 5.1, Bruker AXS Inc., Madison, Wisconsin, USA, 1997.
- [19] G.M. Sheldrick, SHELXL-93, Program for crystal structure determination, University of Göttingen, Germany, 1993.

- [20] G.M. Sheldrick, *Acta Crystallogr. A* 46 (1990) 467.
- [21] G.M. Sheldrick, *SHELXL-93*; Program for crystal structure determination. University of Göttingen, Germany, 1993. Refinement on F_o^2 for all reflections (all of these having $F_o^2 \geq 3\sigma(F_o^2)$). Weighted R -factors wR_2 and all goodnesses of fit S are based on F_o^2 ; conventional R -factors R_1 are based on F_o , with F_o set to zero for negative F_o^2 . The observed criterion of $F_o^2 > 2\sigma(F_o^2)$ is used only for calculating R_1 and is not relevant to the choice of reflections for refinement. R -factors based on F_o^2 are statistically about twice as large as those based on F_o , and R -factors based on all data will be even larger.
- [22] S. Burger, B. Therrien, G. Süß-Fink, *Eur. J. Inorg. Chem.* (2003) 3099.
- [23] K.R. Campos, M. Journet, S. Lee, E.J. Grabowski, R.D. Tillyer, *J. Org. Chem.* 70 (2005) 268.
- [24] The individual phenyl group proton ABC-spin systems were identified but their assignment to a specific auxiliary phenyl group was arbitrary. The absolute identity cannot be assigned as the spatial relation of the phenyl groups to the backbone protons are too similar to be distinguished.
- [25] The Campos structure did not undergo an absorption correction in its refinement, which could improve its R -factor. However, we are inclined to have more confidence in the final model we obtained, although the differences between the two models are subtle.
- [26] Complex $\text{Pd}(\text{PPh}_3)_2(\text{OAc})_2$ was not used as it has been shown to spontaneously autoreduce to form Pd(0) complexes and $\text{O}=\text{PPh}_3$. However, it is noted that in the presence of excess PPh_3 , the reduction potential of $\text{Pd}(\text{PPh}_3)_2(\text{OAc})_2$ has been reported as -1.18 V (vs. SCE) in DMF.
- [27] $\text{Pd}(\text{PPh}_3)_2\text{Cl}_2$ also shows an irreversible oxidation peak on the reverse scan (-2.2 V to $+1.0$ V) at $+0.124$ V which characterized the complex generated by the reduction at -1.25 V. Similar results have been observed with carbene–palladium(II) and mixed carbene/phosphane–palladium(II) complexes. See J. Pytkowicz, S. Roland, P. Mangeney, G. Meyer, A. Jutand, *J. Organomet. Chem.* 678 (2003) 166.